7-2012

Synchronous Oscillatory Solutions in a Two Patch Predator-Prey Model

Matthew H. Becker
College of William and Mary

Synchronous Oscillatory Solutions
In a Two Patch
Predator-Prey Model

A thesis submitted in partial fulfillment of the requirement
for the degree of Bachelors of Science in Mathematics from
The College of William and Mary

by

Matthew H. Becker

Accepted for honors

Junping Shi, Director

Leah Shaw

Daniel Vasiliu

Gexin Yu

Williamsburg, VA
April 25, 2012

Synchronous Oscillatory Solutions in a Two Patch Predator-Prey Model

Matthew H. Becker

Department of Mathematics,

College of William and Mary,

Williamsburg, VA 23187-8795, USA

Email: mhbecker@email.wm.edu

April 20th, 2012

Abstract

A coupled two-patch Rosenzweig-MacArthur system of predator-prey interaction is investigated. Synchronization is the process in which oscillations attain the same frequency based on their coupling. The Moran Effect, the name for the seemingly random changes seen in nature, has been attributed as a cause of synchrony, while scholars have studied other influences to ascertain causal relationships between any of them and a synchronous solution. We use a correlation function similar to Pearson's Correlation, one of the most well known correlation measures in statistical analysis, to measure the synchrony and consider what factors have greater influences upon a synchronous oscillatory solution.

Contents

List of Figures

Chapter 1

Introduction

1.1 Background

In nature there is a constant struggle for survival between species. There are many different forms of engagement, with predation one of the most prevalent and well-known. Predation describes the behavior of two species, a predator and its prey, in which individuals of one species eat those of the other. A predator is the species that gains from the interaction, while the prey is the species that is harmed. The predation directly affects the prey while the abundance of the prey directly affects the predator. This interaction can be modeled to better understand the dynamics of the interaction and coexistence.

A predator species is normally one that contains many fewer individuals, while the number of prey species individuals is generally much larger. The prey species needs to be larger in order to cope with the daily deaths of individuals at the predator's hands. The predator species is often larger than the prey, as in the case of the Lynx and the Snowshoe Hare, yet there are cases, such as the hyena and gazelle in Africa, or particular species of mites consuming each other, in which the prey species is actually bigger [15, 10]. In these cases it might take multiple predators to take down one prey, yet that individual will provide a more substantial feast and hunting occurs much less often. The population

of the predator species often follows the population of the prey with a slight time lag [3]. When the prey population begins to increase, the predator will as well, and the same will happen if the prey population decreases.

Predator-Prey models are differential or difference equations that describe the interaction between two species. The models which we are going to study are all differential equations. A differential equation is an equation that compares one or many variables to a derivative of one such variable. In a first order equation with respect to time, the rate of change of one variable is set equal to an expression containing at least that variable. Predator-Prey models include equations for each of the predator and the prey. The equations are used to study the dynamical behavior of the interacting species.

The first predator-prey models were conceived of by both Alfred J. Lotka and Vito Volterra [14, 22]. Volterra was helping his daughter's fiance, Humberto D'Ancona, to study predatorial fish in the Adriatic Sea while Lotka was attempting to describe oscillations in a chemical reaction. This original model, called the Lotka-Volterra model, is shown as

$$\begin{cases} \dfrac{dN}{dt} = aN - bNP, \\ \dfrac{dP}{dt} = cNP - dP. \end{cases} \tag{1.1}$$

with the population densities of the prey and predator as N and P. Here a is the birth rate of the prey, while d is the death rate of the predator, with b and c the parameters for the change due to interaction between the two species.

Since then there have been many changes and adaptations to these equations, most notably changing two major assumptions. Lotka and Volterra's equations assume that the prey population will grow with no bounds if there is no predator present. Additionally, it is assumed that the predator will always increase prey consumption when there is a larger abundance of prey. Neither of these are the case in nature, and so these had to be addressed and amended. C.S. Holling, a man credited as one of the founders of ecological economics, came up with the idea of changing the functional response, in which the per

capita rate of consumption of the prey by the predator is not linear in prey density, but bounded [8]. His three types of functional responses, now called *Holling Type I, II, and III* functional responses are now a staple in predator-prey modeling.

One very well-known predator-prey model was created by the two-man team of Rosenzweig and MacArthur [19]. This incorporates a *Holling Type II* functional response and is written as

$$\begin{cases} \dfrac{dU}{ds} = \gamma U\left(1 - \dfrac{U}{K}\right) - \dfrac{CMUV}{A+U}, \\ \dfrac{dV}{ds} = -DV + \dfrac{MUV}{A+U}. \end{cases} \tag{1.2}$$

with U and V as the two populations, K as the carrying capacity of the prey, M as the predation rate of the predator as part of the term $\dfrac{MUV}{A+U}$ which measures the interaction between the species with $\dfrac{U}{A+U}$ as the *Holling Type II* functional response, D as the predator death rate, C as the loss in prey, and γ as the birth rate of the prey. We note that the prey follows logistic growth in the absence of a predator.

These models only deal with one area inhabited by predators and prey. In nature it is not the case that a group or population will always stay put and thus it is important to study the dynamics of multiple patches. A two-patch predator prey model incorporates an added term with a diffusion parameter that allows for populations of both predator and prey to move back and forth between two areas of inhabitance.

1.2 Synchrony

A predator-prey interaction model often yields a stable prey-only or coexistence equilibrium solution whose dynamics have been studied and understood thoroughly. The oscillatory solutions due to limit cycles continue to be studied. In the two patch model, there are two independent population patches that are coupled due to diffusion. This leads to the potentiality for synchronization between patches. Synchronization is defined as "adjustment of rhythms of self-sustained periodic oscillators due to their weak inter-

action" [16]. Coupled oscillators operating in synchrony are possibly most well-known in examples of pendulum clocks swaying together or fireflies flashing together in the dark night sky. Another is the human tendency to sleep when its dark and be awake while it is bright [4]. In terms of a predator-prey model, what is meant is the synchrony of oscillation of populations between the two patches.

Several scholars have studied synchrony in predator-prey oscillations. Goldwyn and Hastings [6] showed that very small changes in the spatial habitat can drastically affect synchrony between patches. They also, in another paper [5], show that synchrony in multiple populations can in fact be detrimental and is much more likely to lead to extinction. The Moran Effect, the name for the correlated density independent natural factors, has been attributed as a cause of synchrony [5, 9, 11, 20], along with the dispersal and diffusion of organisms. This random fluctuation, whether determined by a change in weather, a natural disaster, or anything else, can reduce the reproductive success of the prey or predator populations and potentially lead to synchrony in that way [17].

This paper will investigate and analyze synchrony in a two-patch model with one of the tools being a Cross Correlation metric. This metric is very similar to Pearson's Correlation, one of the most widely used correlation measures in statistical analysis [18]. Pearson's Correlation is discrete, using summations, while this metric is continuous using integration. This gives a measurement of how synchronized the populations are to each other. Cross correlation functions are used for a variety of systems, including the study of Alzheimer's disease [1]. Using this tool, we analyze how and why the system moves towards and away from synchrony. Our Cross Correlation metric gives a result which is scaled between -1 and 1, with 1 being fully synchronous, 0 asynchrony, and -1 anti-synchrony. It is defined by

$$cc(u, w; T) = \frac{\langle u(t) - \bar{u}, w(t) - \bar{w} \rangle}{\sigma_u \sigma_w}. \tag{1.3}$$

Here the two functions $u(t)$ and $w(t)$ are the prey solutions in the time span $[0, T]$ for $T > 0$ to the predator-prey model above. $\bar{u}$ and $\bar{w}$ are defined as the average value of

each function over $[0, T]$, with $\bar{u} = T^{-1} \int_0^T u(t)dt$. The numerator is akin to a vector inner product on $L^2(0, T)$, which is

$$\langle f, g \rangle = \int_0^T f(t) \cdot g(t)dt.$$

σ_u is the standard deviation of function u, and it is defined as follows: $\sigma_u = \sqrt{\int_0^T (u - \bar{u})^2(t)dt}$.

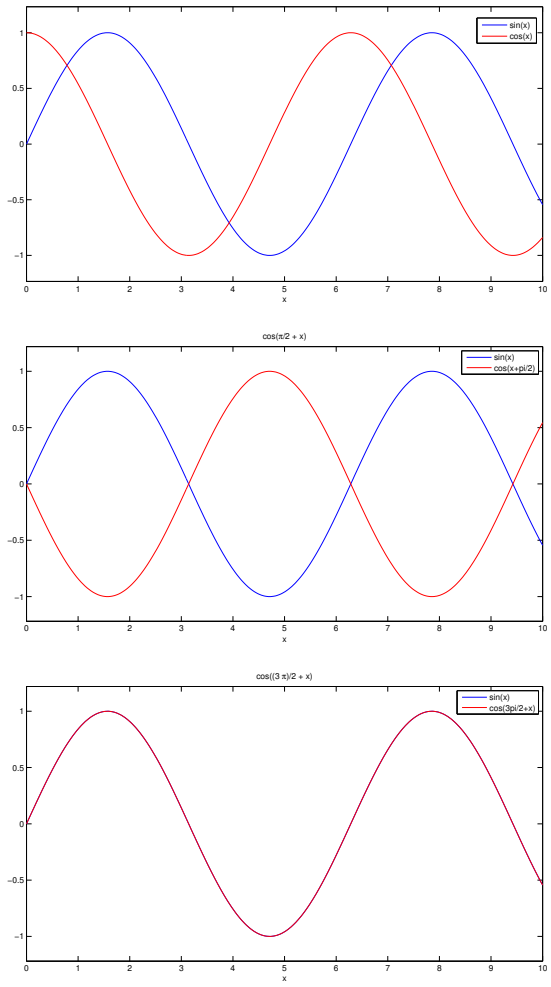

Figure 1.1: Upper: Sine and Cosine curves out of phase. Middle: Sine and Cosine curves with a shift of $\frac{\pi}{2}$. Lower: Sine and Cosine curves with a shift of $\frac{3\pi}{2}$

Cross-Correlation values give a good indication of the synchrony of a pair of solutions, but it cannot decipher whether a system might be locked out of phase. In order to analyze more we apply an arbitrary time shift to the correlation. This is defined as

$$cc_\tau(u, w; T) = \frac{\langle u(t) - \bar{u}, w(t-\tau) - \bar{w} \rangle}{\sigma_u \sigma_w} \tag{1.4}$$

with the numerator being the new vector inner product with a shift

$$\langle f, g \rangle_\tau = \int_0^T f(t) \cdot g(t-\tau) dt.$$

We define the integral to begin at $t = 0$ even though $g(-\tau)$ is not defined because f and g are assumed to be periodic in $\mathbf{R}$ as they can be periodically extended beyond $[0, T]$.

We use a few plots to show the way the time shifts work. Fig. 1.1 contrasts three similar plots. The first shows a simple sine curve and cosine curve. The cross correlation value between the two is 0, since they are perfectly asynchronous. The second plot shows the same sine curve but the cosine curve has been shifted by $\tau = \frac{\pi}{2}$. The correlation value here is -1, with the two curves being fully antisynchronous. The lowest plot shows sine and cosine with a shift of $\tau = \frac{3\pi}{2}$. This synchronizes the two curves and the cross correlation value is exactly 1.

1.3 Dynamics

For a system of differential equations with dimension 2, the Poincaré-Bendixson Theorem [2] tells that the typical behavior of a bounded and autonomous system is either to converge to an equilibrium or go to a periodic orbit.

In predator-prey dynamics, we often look for equilibria which we can analyze. Equilibrium points are solutions to differential equations in which all the time derivatives are zero. The trivial equilibrium is extinction for all species. It is easy to understand intuitively that this would be an equilibrium solution, yet is not useful for what we are looking

for. The most important equilibrium point is the coexistence equilibrium, that solution in which both predator and prey are able to survive.

One important type of solution for us is called a periodic orbit. This is the case when the populations in each patch oscillate back and forth between larger and smaller populations systematically. The system is said to be locked in orbit where within a certain time period the oscillation will continue again, much like a well known sine or cosine curve.

This paper will use a form of the Rosenzweig-MacArthur model to study synchronous oscillations in a two-patch system.

1.4 Results

We began with the one patch model, and we studied the stability of the system. For the two patch model, we determined parameters necessary for the existence of an asymmetric periodic orbit and were able to then extrapolate that into the two patch case. The orbit is asymmetric if we have $u \not\equiv w$ and $v \not\equiv x$, otherwise we call it a symmetric periodic orbit. We studied the symmetry of simultaneous orbits in distinct patches when we allow for diffusion between the two, mostly maintaining a relatively small predator death rate η.

We have found that synchrony, as quantified by our cross correlation function, depends upon our initial conditions and also the diffusion coefficients. When a system initially is closer to synchrony, it will tend to go to synchrony quickly. Additionally, the presence of large diffusion parameters, in essence allowing for many of the population to move quickly between patches, will lend to synchronization of the system.

We also can see that the cross correlation function for the predator-prey model usually does not achieve a value of -1, which we call antisynchrony. We know that by observation that autocorrelation for most periodic functions cannot actually attain the entire range $-1 \leq f(x) \leq 1$. As an example we can look at the function $f(x) = \sin(x) + \sin(2x)$ with a period of 2π. The autocorrelation function with time shift for this function is calculated

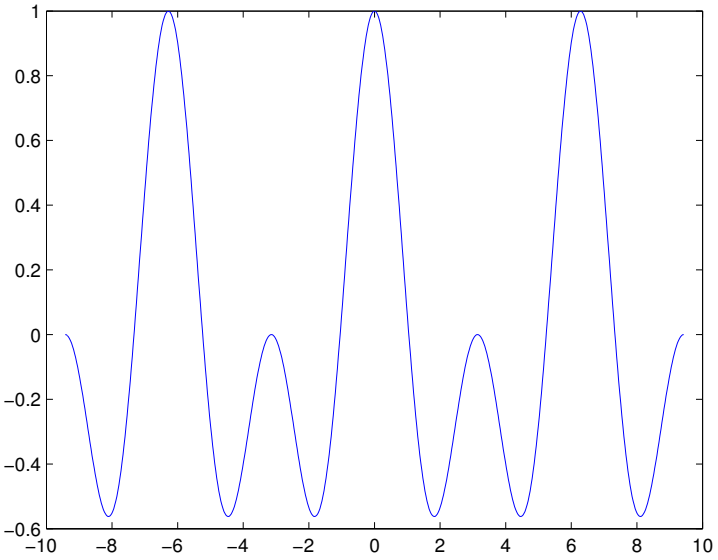

Figure 1.2: Plot of $\dfrac{\cos(\tau)+\cos(2\tau)}{2}$

as

$$cc(\tau, f) = \frac{\int_{-\pi}^{\pi} f(x) \cdot f(x-\tau)dx - 2\pi(\bar{f})^2}{\int_{-\pi}^{\pi} f^2(x)dx - 2\pi(\bar{f})^2}$$

for an arbitrary time shift $0 < \tau < 2\pi$ that will be discussed in more detail in Chapter 3. We know that the average value of this function is 0 so we have

$$cc(\tau, f) = \frac{\int_{-\pi}^{\pi} f(x) \cdot f(x-\tau)dx}{\int_{-\pi}^{\pi} f^2(x)dx}.$$

When we integrate this function we find $cc(\tau, f) = \dfrac{\pi(\cos(x)+\cos(2x))}{\pi \cdot 2}$ and so $cc(\tau, f) = \dfrac{\cos(\tau)+\cos(2\tau)}{2}$. Now, we can see from the plot in Fig. 1.2, that this autocorrelation function cannot reach -1 and so there can never be any antisynchrony. We will generalize this in Section 3.3.

Chapter 2

Mathematical Analysis

2.1 One Patch Model

Before beginning to study a two-patch system of equations, we must first look at a single patch model. There are many forms and variations of predator-prey models, so we chose to work with a model by Alan Hastings found in his paper in Ecology Letters in 2001 [7]; the model is a slight variation of the Rosenzweig-MacArthur model.

$$\begin{cases} \dfrac{du}{dt} = u\left(1-\alpha u\right) - \dfrac{uv}{1+\beta u}, \\ \dfrac{dv}{dt} = \dfrac{uv}{1+\beta u} - \eta v \end{cases} \tag{2.1}$$

In this equation, $\frac{du}{dt}$ and $\frac{dv}{dt}$ represent the rates of change of $u(t)$, the prey population, and $v(t)$, the predator population, respectively. This basic model considers the growth, death, and interaction of the populations. The term $u(1-\alpha u)$ represents the prey's growth rate while $\frac{uv}{1+\beta u}$ is a Holling Type II Functional Response measuring the interaction between the predator and prey. This model represents a logistic growth of the prey when there is no predator present. As we can see from the equations, the interaction term is negative for the prey while is positive for the predator, showing what we assume to be true that the predator gains from the interaction while the prey is harmed. The final term ηv is a

simple intrinsic death rate of the predator.

There are multiple equilibria present, including the trivial equilibrium $(0, 0)$, and the semi-trivial equilibrium $(\frac{1}{\alpha}, 0)$, yet what is most important is the coexistence equilibrium, in which both species survive. Our coexistence equilibrium is (λ, v_λ) for $\lambda = \frac{\eta}{1-\beta\eta}$ and $v_\lambda = (1-\alpha\lambda)(1+\beta\lambda)$. Through linearization we construct the Jacobian for this equilibrium point to be

$$J(\lambda, v_\lambda) = \begin{pmatrix} \frac{\lambda(\beta-\alpha-2\alpha\beta\lambda)}{1+\beta\lambda} & \frac{-\lambda}{1+\beta\lambda} \\ \frac{1-\alpha\lambda}{1+\beta\lambda} & 0 \end{pmatrix}. \tag{2.2}$$

We calculate the Trace and Determinant of this Jacobian matrix to be

$$Tr = \frac{\lambda(\beta-\alpha-2\alpha\beta\lambda)}{1+\beta\lambda}, \tag{2.3}$$

and

$$Det = \frac{\lambda(1-\alpha\lambda)}{(1+\beta\lambda)^2}. \tag{2.4}$$

The characteristic equation for eigenvalues is $\mu^2 - Tr\mu + Det = 0$. We use μ for the eigenvalues since the standard λ is being used in the equations above. When $Tr = 0$, we have $\mu^2 = -Det$. This will give a Hopf Bifurcation when the determinant is positive. Since $Tr = \frac{\lambda(\beta-\alpha-2\alpha\beta\lambda)}{1+\beta\lambda}$, we have $\frac{\lambda(\beta-\alpha-2\alpha\beta\lambda)}{1+\beta\lambda} = 0$ and subsequently $\lambda = \frac{\beta-\alpha}{2\alpha\beta}$. We see that when $0 < \lambda < \frac{\beta-\alpha}{2\alpha\beta}$ a periodic orbit will occur. Since $\lambda = \frac{\eta}{1-\beta\eta}$, we fix our parameters such that $\frac{\eta}{1-\beta\eta} < \frac{\beta-\alpha}{2\alpha\beta}$. Additionally, since λ must be positive, we have $\beta > \alpha$.

Figures $2.1 - 2.3$ show phase portraits for three possible solutions for the one patch system. The red curves are nullclines, with the blue being solution curves. Fig. 2.1 shows that when $\lambda > \frac{1}{\alpha}$, the solutions of the system tend to the semi-trivial equilibrium $(\frac{1}{\alpha}, 0)$ for many different initial conditions. This is when the predator goes extinct and the prey goes to its carrying capacity. In Fig. 2.2 we see that when $\frac{1}{\alpha} > \lambda > \frac{\beta-\alpha}{2\alpha\beta}$, the

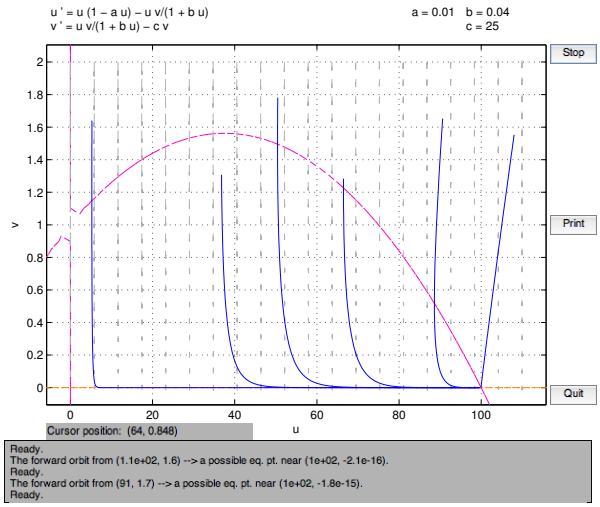

Figure 2.1: One Patch Phase Portrait. Here $\lambda > \dfrac{1}{\alpha}$

system goes to the coexistence equilibrium that we call (u^*, v^*), and prey and predator both survive and go to a lasting equilibrium population. Finally, when $\dfrac{\beta - \alpha}{2\alpha\beta} > \lambda > 0$ Fig. 2.3 has a periodic orbit, where both predator and prey survive but their populations oscillate around the equilibrium point (u^*, v^*).

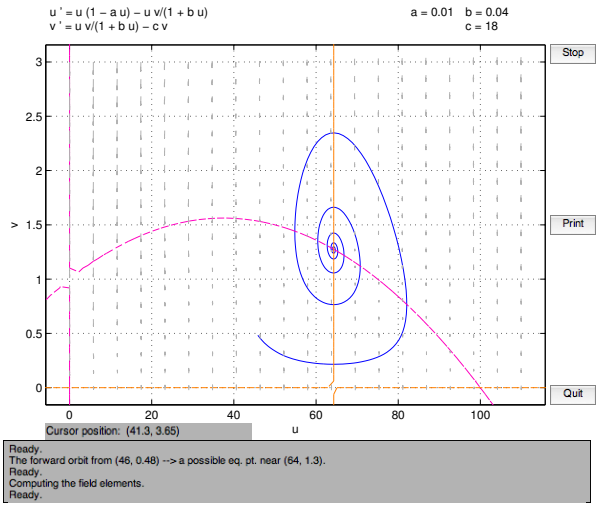

Figure 2.2: One Patch Phase Portrait. Here $\frac{1}{\alpha} > \lambda > \frac{\beta - \alpha}{2\alpha\beta}$

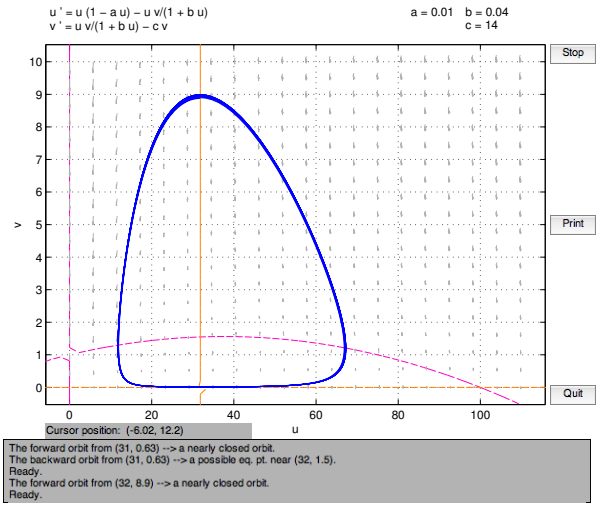

Figure 2.3: One Patch Phase Space. Here $\frac{\beta - \alpha}{2\alpha\beta} > \lambda > 0$

These plots are generated by setting the parameters such that $\lambda > \frac{1}{\alpha}$, $\frac{1}{\alpha} > \lambda > \frac{\beta - \alpha}{2\alpha\beta}$, and $\lambda < \frac{\beta - \alpha}{2\alpha\beta}$, respectively. We do this by keeping $\alpha = 0.01, \beta = 0.04$ and then $\eta = 25$

in Fig. 2.1, $\eta = 18$ in Fig. 2.2, and $\eta = 14$ in Fig. 2.3.

The dynamics of a single patch model have been studied and analyzed over time and the stability of the equilibria is readily apparent. What this model lacks, however, is the capacity to analyze behavior and dynamics should the species, or members of it, move between multiple locations. This brings about the necessity for a multiple patch model.

2.2 Two Patch Model

A two patch model, unlike a single patch model, is a system of four ordinary differential equations. For each patch, or geographic habitat, a certain amount of prey and predator inhabit the area. Their interaction, growth, and decay are modeled by a one patch model for each patch, but with an extra term. This addition is a term that allows for predator and prey to move back and forth between the two patches. When this is included, the patches are said to be coupled.

We use the same one patch model as (2.1) and with the addition of coupling, we have the system as introduced in [7]:

$$\begin{cases} \dfrac{du}{dt} = f_1(u,v) + a(w-u), \\ \dfrac{dv}{dt} = g_1(u,v) + b(x-v), \\ \dfrac{dw}{dt} = f_2(w,x) - a(w-u), \\ \dfrac{dx}{dt} = g_2(w,x) - b(x-v), \end{cases} \tag{2.5}$$

where for $i = 1, 2$,

$$f_i(u,v) = u\,(1-\alpha_i u) - \frac{uv}{1+\beta_i u}, \quad g_i(u,v) = \frac{uv}{1+\beta_i u} - \eta_i v. \tag{2.6}$$

In this system, u and w are the prey in each patch and v and x are the predator in each patch, respectively. The functions $f_i(u,v)$ and $g_i(u,v)$ are the prey and predator equations from the single patch model. a and b are our diffusion parameters; these govern

the extent of the diffusion, or migration, between patches. We see if $\alpha_1 = \alpha_2, \beta_1 = \beta_2$, and $\eta_1 = \eta_2$ then we have two homogeneous patches, while if the parameters are unequal, the patches are considered heterogeneous. We only consider the homogeneous patches in this paper.

2.3 Linearization and Stability Analysis of the Symmetric Case

The coexistence equilibrium from the one patch model is vital for the two patch model. To study this, we must first apply a transformation to our spacially homogenous system by manipulating our four population variables [12]. We take sums and differences of the variables to create

$$\begin{cases} U = u + w, \\ V = v + x, \\ W = u - w, \\ X = v - x, \end{cases} \tag{2.7}$$

with U and V the sums of the predators and prey in the two patches, while W and X are the differences. We are able to produce a new system that models the behavior of the sums and differences of the populations

$$\begin{cases} U' = f\left(\frac{U+W}{2}, \frac{V+X}{2}\right) + f\left(\frac{U-W}{2}, \frac{V-X}{2}\right), \\ V' = g\left(\frac{U+W}{2}, \frac{V+X}{2}\right) + g\left(\frac{U-W}{2}, \frac{V-X}{2}\right), \\ W' = f\left(\frac{U+W}{2}, \frac{V+X}{2}\right) - f\left(\frac{U-W}{2}, \frac{V-X}{2}\right) - 2aW, \\ X' = g\left(\frac{U+W}{2}, \frac{V+X}{2}\right) - g\left(\frac{U-W}{2}, \frac{V-X}{2}\right) - 2bX, \end{cases} \tag{2.8}$$

Our coexistence equilibrium (λ, v_λ) in one patch model must be converted into our new system. The coexistence equilibrium (U, V, W, X) will be $(2\lambda, 2v_\lambda, 0, 0)$. The Jacobian for

this new equilibrium is a 4×4 matrix which can be constructed quite simply. The zeroes in the equilibrium mean that this will be a block matrix of the form

$$J = \begin{pmatrix} \frac{\lambda(\beta - \alpha - 2\alpha\beta\lambda)}{1+\beta\lambda} & \frac{-\lambda}{1+\beta\lambda} & 0 & 0 \\ \frac{1-\alpha\lambda}{1+\beta\lambda} & 0 & 0 & 0 \\ 0 & 0 & \frac{\lambda(\beta - \alpha - 2\alpha\beta\lambda)}{1+\beta\lambda} - 2a & \frac{-\lambda}{1+\beta\lambda} \\ 0 & 0 & \frac{1-\alpha\lambda}{1+\beta\lambda} & -2b \end{pmatrix} \tag{2.9}$$

The upper left block is simply the Jacobian we constructed for the coexistence equilibrium of one patch model, while the lower right block is very similar but with the terms $2a$ and $2b$ subtracted from the entries in the main diagonal, respectively.

We see that our Jacobian is of the form:

$$J = \begin{pmatrix} B_1 & 0 \\ 0 & B_2 \end{pmatrix} \tag{2.10}$$

The trace and determinant of B_1 have already been calculated in the one-patch section, since B_1 is simply the Jacobian for the One-Patch Model. We calculate the trace and determinant of B_2 and see that

$$Tr(B_2) = \frac{\lambda(\beta - \alpha - 2\alpha\beta\lambda)}{1+\beta\lambda} - 2a - 2b, \tag{2.11}$$

and

$$Det(B_2) = \frac{(-2b)\lambda(\beta - \alpha - 2\alpha\beta\lambda)}{1+\beta\lambda} + 4ab + \frac{\lambda(1-\alpha\lambda)}{(1+\beta\lambda)^2}. \tag{2.12}$$

We simplify the form by calling $h_1(\lambda) = \frac{\lambda(\beta - \alpha - 2\alpha\beta\lambda)}{1+\beta\lambda}$ and $h_2(\lambda) = \text{Det}(B_2)$. We can see that $h_1(0) = 0 = h_1(\frac{\beta - \alpha}{2\alpha\beta})$ and there is a λ_* such that $h_1'(\lambda_*) = 0$, the λ-value for which the maximum value occurs. When $\text{Tr}(B_2) = 0$ and $\text{Det}(B_2) > 0$ we have the necessary conditions for a Hopf bifurcation. The Hopf bifurcation points occur where the parabola-like curve $y = h_1(\lambda)$ intersects with the line $y = 2(a+b)$. As long as $\text{Det}(B_2) > 0$, we see that when $h_1(\lambda_*) > 2(a+b)$ we have two bifurcation points. We see this since that

condition makes it possible for the trace of B_1 to be equal to 0. When $\mathrm{Det}(B_2) = 0$ we have a steady state bifurcation.

The graph of $h_1(\lambda)$ with $\alpha = 0.01$ and $\beta = 0.04$ is shown below in Fig. 2.4. The intersections between the line $2(a+b)$ and this curve are the Hopf bifurcation points so we can see under what conditions we will have $0, 1$, or 2 Hopf bifurcation points. For this case, we must have $2(a+b) \leq 0.15$ in order to have two bifurcation points.

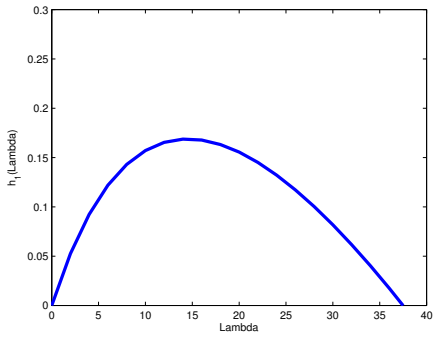

Figure 2.4: Plot of λ vs. $h_1(\lambda)$. Here $\alpha = 0.01$ and $\beta = 0.04$.

When $\lambda \geq \dfrac{\beta - \alpha}{2\alpha\beta}$ the system goes to equilibrium almost invariably. On the other hand, when $0 < \lambda < \dfrac{\beta - \alpha}{2\alpha\beta}$ it depends slightly more on the initial condition. If the system is close to symmetry then it will likely go to a limit cycle, while if not then it might never become synchronous and exhibit seemingly chaotic behavior.

2.4 Bifurcation Plots

The bifurcation plots in Fig. 2.5 shows similar dynamics to our own system. These two plots are from a Rosenzweig-MacArthur model studied by Yuanyuan Liu [13]:

$$\begin{cases} u' = f_1(u,v) + a(w-u), \\ v' = g_1(u,v) + c(x-v), \\ w' = f_2(w,x) - a(w-u), \\ x' = g_2(w,x) - c(x-v), \end{cases} \tag{2.13}$$

where for $i = 1, 2$,

$$f_i(u,v) = u\left(1 - \frac{u}{K_i}\right) - \frac{m_i uv}{1+u}, \quad g_i(u,v) = \frac{m_i uv}{1+u} - e_i v. \tag{2.14}$$

These plots can be created using `Matcont` in `Matlab`. These are two separate bifurcation plots for different parameters showing different phenomena. Each plots the bifurcation parameter e against the prey u, although the top plot is against $max(u)$. BP stands for branch point, H for Hopf bifurcation, NS for Neimark-Sacker bifurcation, LPC for limit point bifurcation of cycles, and bPC for branch point of cycles. We are interested in the branch points and Hopf bifurcations. We can see in the plot on the top the symmetric equilibrium curve, $(u(t), v(t), x(t), w(t)) = (\lambda, v_\lambda, \lambda, v_\lambda)$ rising from the trivial equilibrium of $u = 0$ as the predator death rate (e in this case) increases. The circuit represents the asymmetric periodic orbit while the branch that goes up and off to the left represents the symmetric orbit. We want to study the asymmetric periodic orbit so we have set our parameters such that η (our version of e) is within the right range to allow for the presence of such an orbit. We will use numerical simulation and cross correlation to further consider the system in the next chapter. The plot on the left exhibits similar dynamics, yet rather than a Hopf bifurcation point leading to a periodic orbit, there is a branching point with another equilibrium curve, and the orbit comes off of that curve.

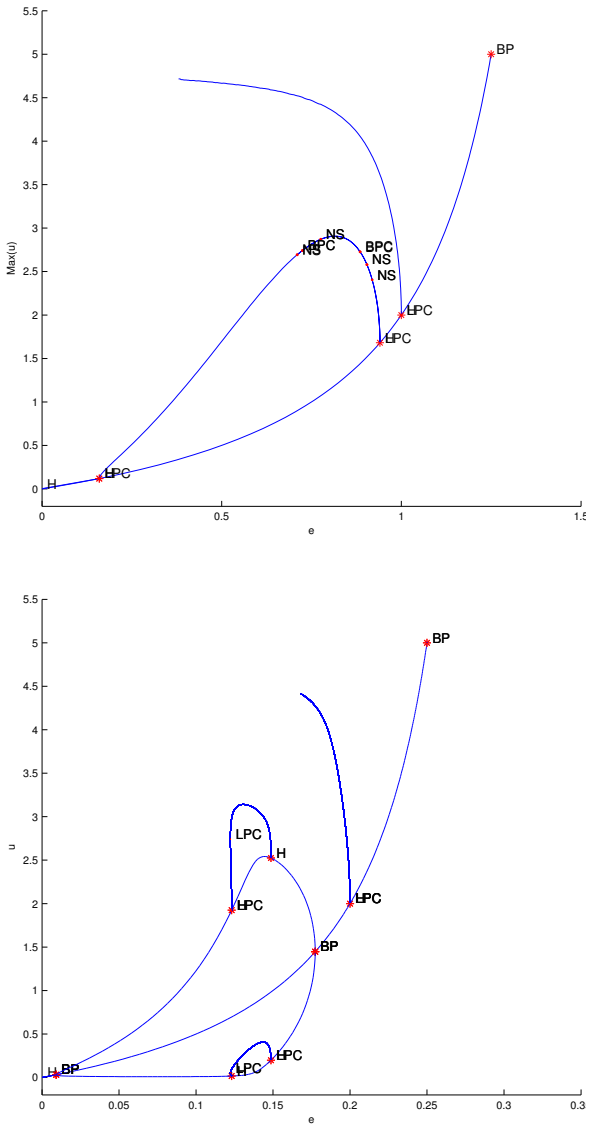

Figure 2.5: Bifurcation Diagrams under parameters from a similar system.

Chapter 3

Numerical Work

Numerical simulations often offer a road map as to what direction the mathematical analysis should be headed. Valuable information can be attained using a more deterministic manner of work. Many illustrate a point or conclusion much more easily than is possible in other ways. The main purpose of our numerical simulations is to study the cross correlation value and how it changes. In this chapter we are fixing the parameters $\alpha_1 = \alpha_2 = 0.01$, $\beta_1 = \beta_2 = 0.04$, $T = 1000$. These are the parameters included in the prey's logistic growth, the predation rate, and time. We are changing the diffusion parameters a and b, as well the predator death rate η, while maintaining $\eta_1 = \eta_2$.

3.1 Impact of Diffusion Coefficient

Figures 3.1 and 3.2 show a way to study the system. The figures show the value of the correlation coefficient and the way it changes due to an increase in diffusion, whether prey or predator. Each plot is drawn with parameters $\alpha_1 = \alpha_2 = 0.01, \beta_1 = \beta_2 = 0.04, \eta_1 = \eta_2 = 1$, and $a = 3b$. The horizontal axis is the diffusion coefficient of prey a (from 0 to 0.03), and the vertical axis is the correlation coefficient values. The cross correlation is calculated beginning at $t = 0$, and so the results measure a combined effect of how things

synchronize given the parameters and initial conditions and also whether they synchronize in the long term for these parameters.

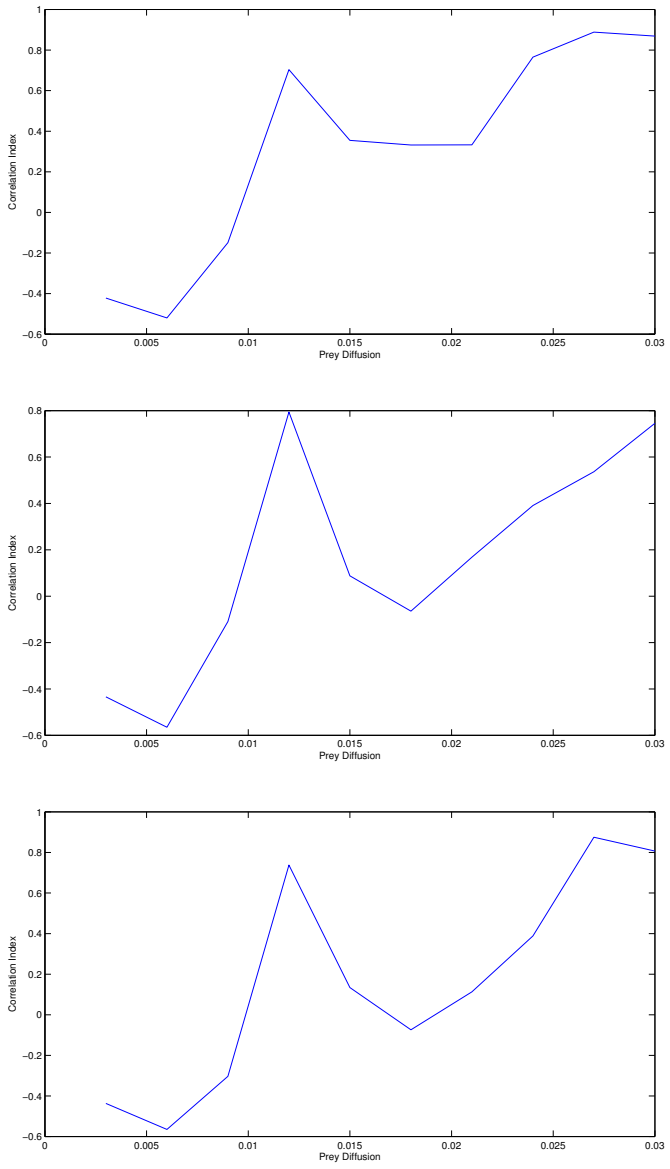

Figure 3.1: Plot of the cross correlation vs. diffusion coefficients. Initial values are ((upper) $u(0) = 4, v(0) = 3, w(0) = 0, x(0) = 0$; (middle) $u(0) = 10, v(0) = 5, w(0) = 0, x(0) = 0$; (lower) $u(0) = 8, v(0) = 2, w(0) = 0, x(0) = 0$.

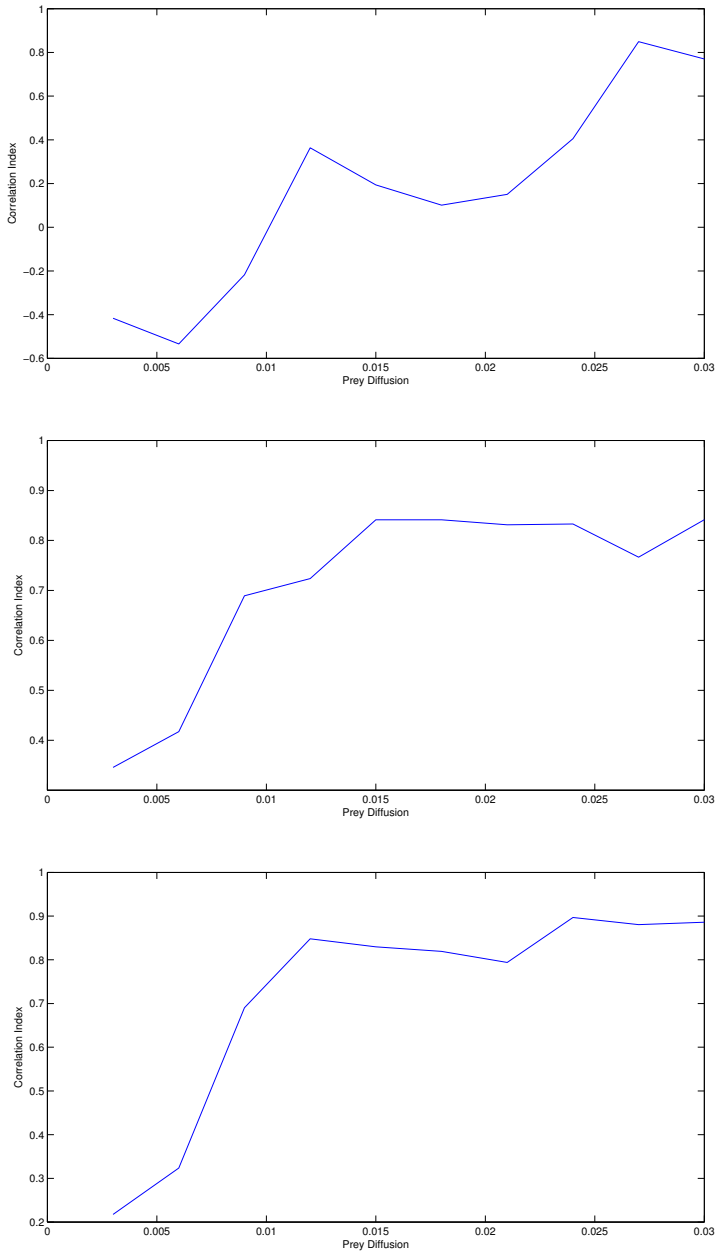

Figure 3.2: Plot of the cross correlation vs. diffusion coefficients. Initial values are ((upper) $u(0) = 10, v(0) = 5, w(0) = 5, x(0) = 2$; (middle) $u(0) = 4, v(0) = 3, w(0) = 3, x(0) = 4$; (lower) $u(0) = 8, v(0) = 6, w(0) = 6, x(0) = 8$.

Figs. 3.1 and 3.2 show similar results from differing initial conditions: as diffusion coefficient increases, cross correlation increases with it, albeit not in a linear way. The cross correlation values jump, and when the initial condition is such that there is no population of either predator or prey in patch 2, the parameters $a = 0.012, b = 0.004$ give an outlying value. Figure 3.2 has initial conditions of populations in both patches. We see, from these 6 plots of cross correlation versus diffusion coefficients that there appears to be a lower bound of -0.6.

The level of synchrony will also depend upon the initial conditions. If the initial values of the two predator or prey populations are close enough to each other then that will lead to synchrony independent of the diffusion rates. Contrastingly, if the initial values are so far from each other then even with large diffusion rates the system may never reach synchrony, or will take a much larger time scale to achieve its long term behavior and synchrony.

Figure 3.3 below shows plots in which the initial conditions are very similar. In the upper plot, we begin with a symmetric initial condition. As we expected, the system remains in perfect synchrony. The middle plot is has an initial condition of almost perfect synchrony, $u(0) = 4, v(0) = 3, w(0) = 4, x(0) = 2.9$. We see that it is asynchronous when the values of the diffusion coefficients are low, but will rise to synchrony relatively quickly. We can contrast that with the lowest plot, with initial conditions $u(0) = 4, v(0) = 3, w(0) = 4, x(0) = 2$ which is still close to synchrony. It exhibits the same shape as those seen above in Figures 3.1 and 3.2, with nothing to suggest that it is so close to synchrony to begin with. This leads to the conjecture that the diffusion coefficients impact synchrony more than the initial conditions, despite the initial conditions having a seen effect.

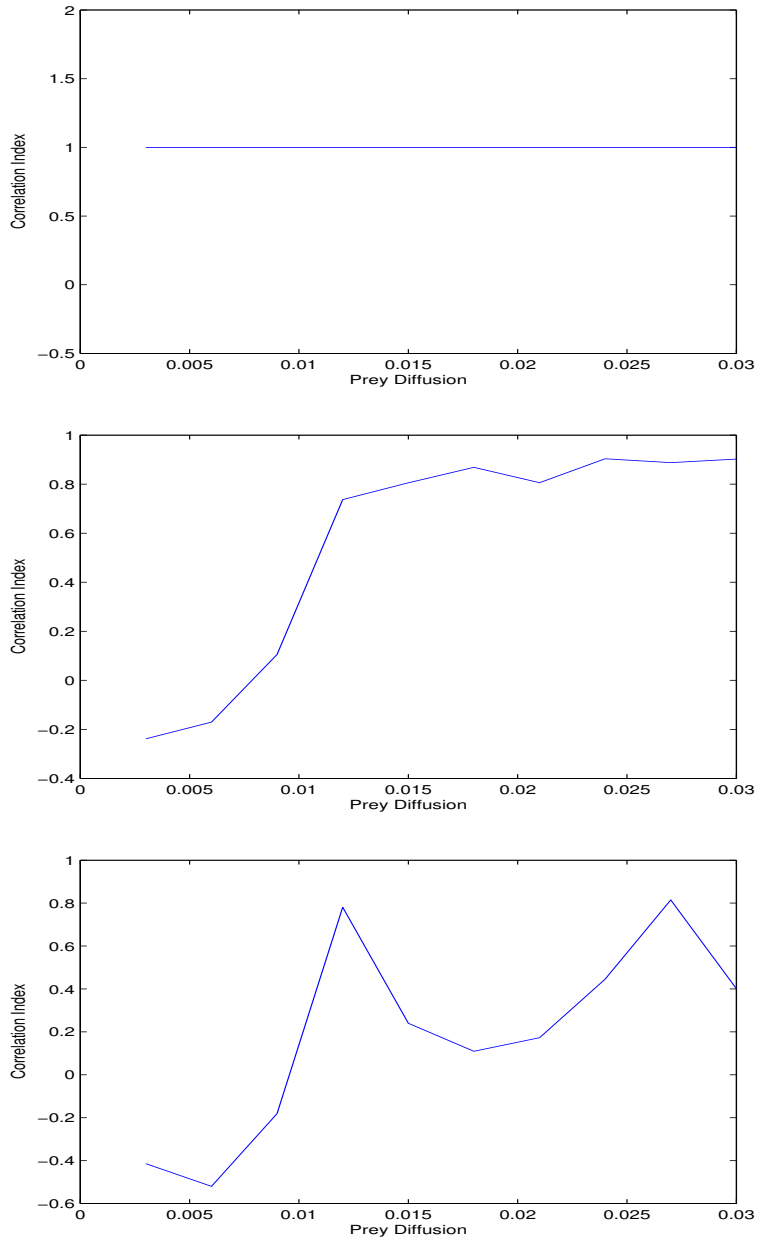

Figure 3.3: Plot of the cross correlation vs. diffusion coefficients. Initial values are ((upper) $u(0) = 4, v(0) = 3, w(0) = 4, x(0) = 3$; (middle) $u(0) = 4, v(0) = 3, w(0) = 4, x(0) = 2.9$; (lower) $u(0) = 4, v(0) = 3, w(0) = 4, x(0) = 2$.

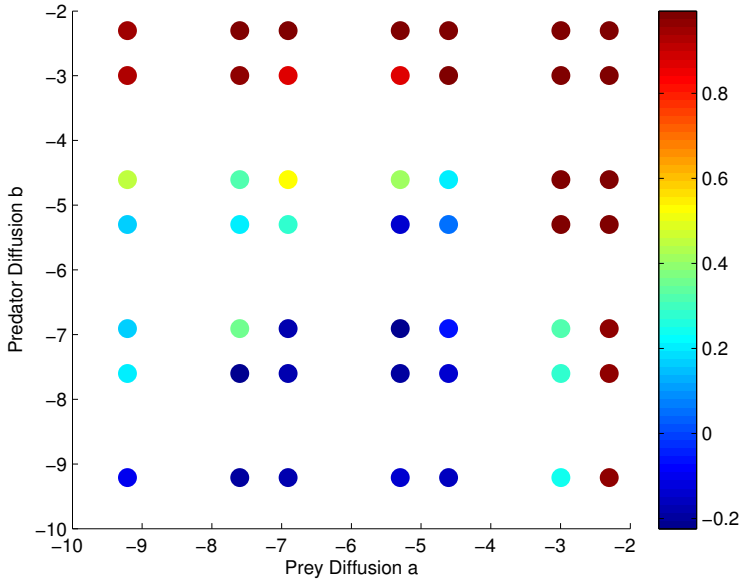

Figure 3.4: Correlation coefficients plotted against predator diffusion a and prey diffusion b. Here $\alpha_1 = \alpha_2 = 0.01$, $\eta_1 = \eta_2 = 1$, $\beta_1 = \beta_2 = 0.04$, $T = 1000$, and $0.0001 \leq a \leq 0.1$, $0.0001 \leq b \leq 0.1$. Initial values are $u(0) = 4, v(0) = 3, w(0) = 0, x(0) = 0$.

These previous plots can be combined, adding more parameter values, into a 3 dimensional scatterplot to make them easier to understand, analyze, and compare. Fig. 3.4 shows the correlation coefficient based on each of the two diffusion rates.

3.2 Lag Synchrony

Rather than simply looking at the correlation coefficient on its own, we can look at the correlation for small time shifts. This will show if the oscillations are locked, either in or out of phase, since a time shift would then eventually give a correlation coefficient very close to 1 once one of the patches has been shifted in time. We study this along with the time series and phase space to give a fuller picture of what is going on. A few

specific examples are studied below. In these examples we are concentrate on the predator without loss of generality, since we were able to see numerically that the prey populations in each will behave similarly. Each of these systems are calculated from $t = 0$, and we have plotted the transient behavior to see how they go to their long term behavior.

The numerical simulation for the initial conditions $u(0) = 4, v(0) = 3, x(0) = 0, y(0) = 0$ and diffusion parameters $a = 0.1, b = 0.001$ is shown in the upper three plots in Fig. 3.5. The time series (upper right) shows the predator populations in each patch. The time series suggests that the two patches are synchronous, and the phase space (upper left) on the corroborates. The graphical representations agree with the cross correlation value of 0.9950, which means that the system is in almost perfect synchrony. The plot of cross correlation versus time shift shows periodicity with an average cross correlation of -3.9401×10^{-4}. The lower three plots in Fig.3.5 are from an asynchronous system that shows some very interesting dynamics. The cross correlation is -0.3066, seemingly one of the lowest possible values. The time series and phase space both show the lack of synchrony, but the phase space also shows an interesting figure 8 shaped orbit. The period appears much shorter than that of the other systems. The time shift plot shows that while the system is not synchronous and the average cross correlation value is 6.6797×10^{-4}, it might just be out of phase and potentially only a very small time shift is needed for the system to become synchronous.

Figures 3.6 shows less synchronous systems tending towards asynchrony. The cross correlation values for $\tau = 0$ are 0.4703 (upper) and 0.6171 (lower), and both time shift plots show that each cannot possibly become synchronous simply by changing the time in one patch. The time series for the upper system shows oscillations that continue to grow over time, while the time series in the lower system shows populations that appear to be in a bursting pattern. Again, the average cross correlation values over all the times shifts are almost exactly zero, with them being -0.0046 and 0.0037.

These plots and figures of solutions provide a useful map for understanding the nature

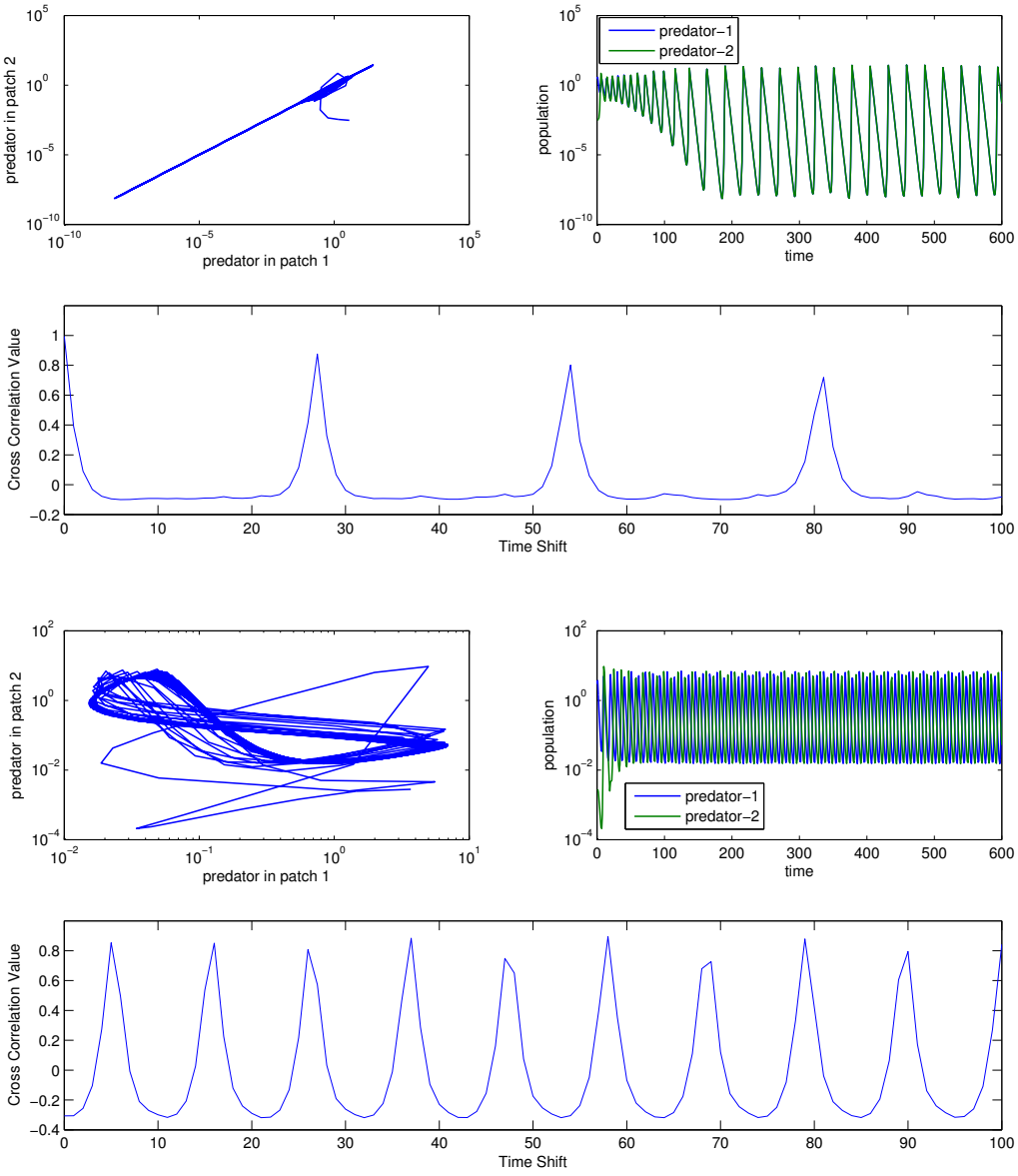

Figure 3.5: Numerical simulation of synchrony. UPPER: $a = 0.1$ and $b = 0.001$. LOWER: $a = 0.001$ and $b = 0.001$ A. (upper left): Phase portrait; B. (upper right): Time Series (Predator vs. time); C. (lower): Cross Correlation vs. Time Shift τ.

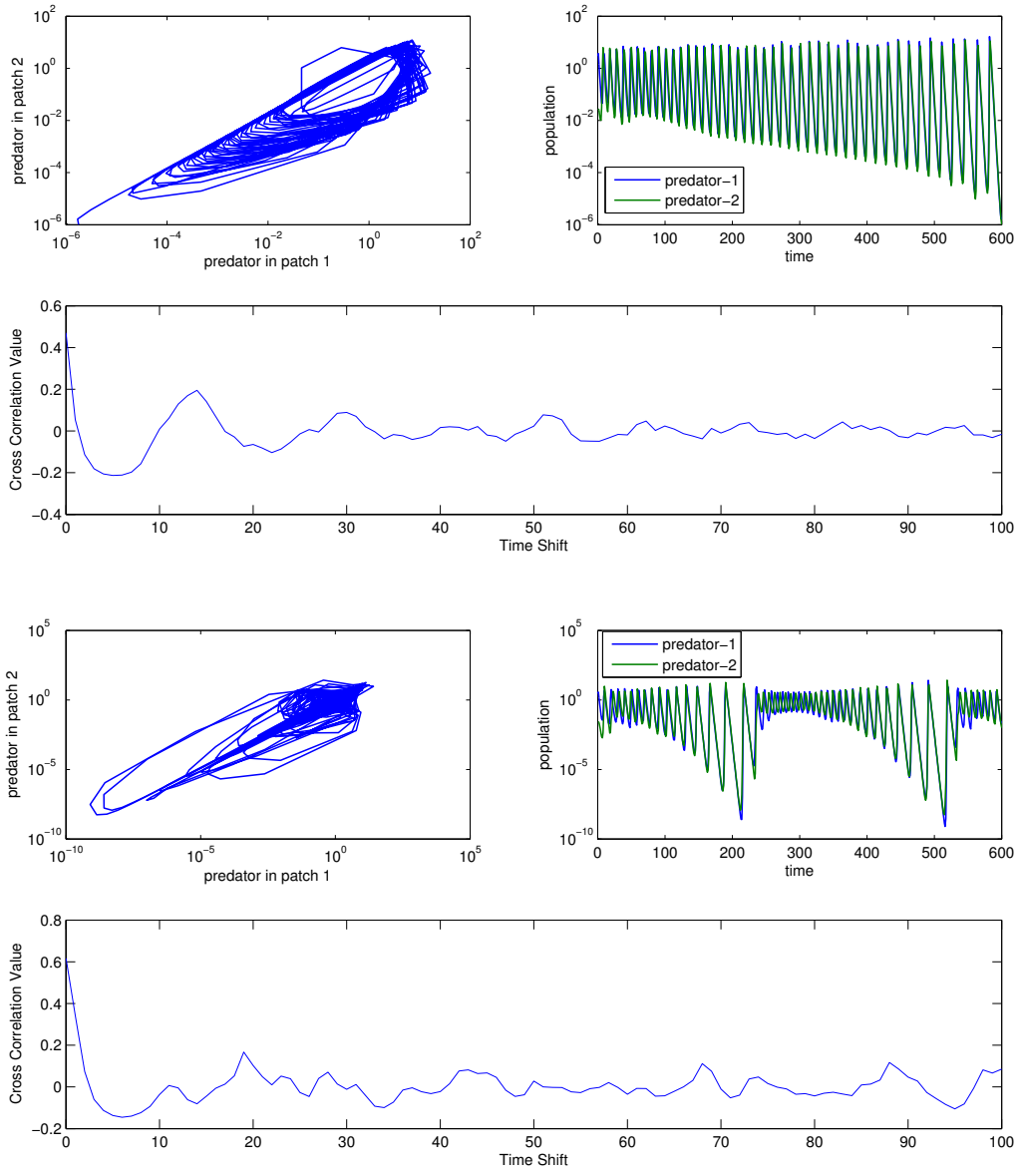

Figure 3.6: Numerical simulation of synchrony. UPPER: $a = 0.01$ and $b = 0.01$. LOWER: $a = 0.1$ and $b = 0.01$ A. (upper left): Phase portrait; B. (upper right): Time Series (Predator vs. time); C. (lower): Cross Correlation vs. Time Shift τ.

of oscillations over a larger time scale. The cross correlation (with or without time shifts) can be compared easily to phase spaces and time series providing invaluable insight not attainable with simple equations and matrices.

We see, from the study of bifurcation points and stability earlier, that if $\eta > 15$ we are likely to head towards a stable equilibrium. This can be seen in the figure below. Fig. 3.7 shows what the three plots look like for a stable equilibrium. Cross correlation is essentially undefined when the time series approaches a constant, since the standard deviation becomes 0.

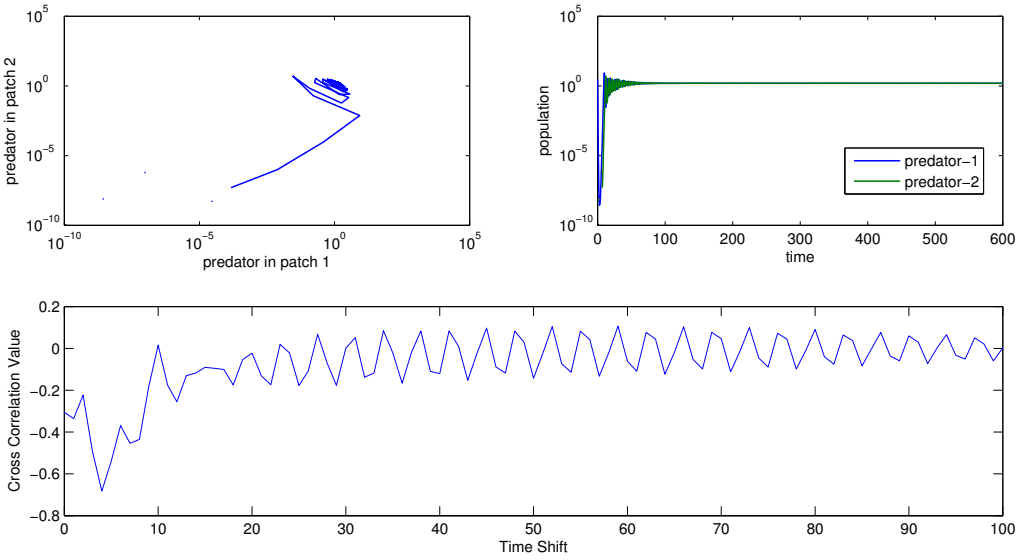

Figure 3.7: Numerical simulation of synchrony. Here $a = 0.001$ and $b = 0.001$. A. (upper left): Phase portrait; B. (upper right): Time Series (Predator vs. time); C. (lower): Cross Correlation vs. Time Shift τ.

3.3 Motivation for Non-Existence of Antisynchrony

The example shown in Chapter 1 in which we showed a specific function could not achieve antisynchrony is generalized in the lemma below. We use this to see our system will not likely achieve antisynchrony.

Lemma: Let $u(t)$ be a periodic function with period 2π. Then $-1 \leq cc(\tau, u) \leq 1$ for $0 < \tau < 2\pi$, and $cc(0, u) = 1$. If $cc(\tau, u) = -1$, then

$$u(t) = \sum_{m=1}^{\infty} [A_m \cos((2m-1)nt) + B_m \sin((2m-1)nt)]$$

for some $n \in \mathbb{N}$, $A_m, B_m \in \mathbf{R}$, and $\tau = \dfrac{(2k-1)\pi}{n}$ for some $k = 1, 2, \ldots$ and $gcd(2k-1, n) = 1$.

Proof. Without loss of generality, we consider the function on the interval $(-\pi, \pi)$. The definition of cross correlation with a time shift for two functions u and w is

$$cc_\tau(u, w; T) = \frac{\langle u(t) - \bar{u}, w(t-\tau) - \bar{w} \rangle}{\sigma_u \sigma_w},$$

with the numerator as

$$\langle f, g \rangle_\tau = \int_{-\pi}^{\pi} u(t) \cdot w(t-\tau) dt.$$

and

$$\sigma_u = \sqrt{\int_{-\pi}^{\pi} (u - \bar{u})^2(t) dt}.$$

We set $u = w$ so we say

$$cc_\tau(u; T) = \frac{\langle u(t) - \bar{u}, u(t-\tau) - \bar{u}_\tau \rangle}{\sigma_u^2}.$$

We use the definition of the inner product and standard deviation to re-write the equation to be

$$cc_\tau(u, T) = \frac{\int_{-\pi}^{\pi} u(t) \cdot u(t-\tau) dt - \int_{-\pi}^{\pi} u(t) \bar{u} dt - \int_{-\pi}^{\pi} u(t-\tau) \cdot \bar{u} dt + (\bar{u})^2 2\pi}{\int_{-\pi}^{\pi} u^2(t) dt - \bar{u}^2 2\pi}.$$

We know that the second term of the numerator can be solved as $\int_{-\pi}^{\pi} u(t)dt = 2\pi\bar{u}$. Also, since $u(t)$ is periodic we have $\int_{-\pi}^{\pi} u(t-\tau)dt = 2\pi\bar{u}$ so those and the second term will now cancel with the fourth term on the numerator so we have

$$cc_\tau(u,\tau) = \frac{\int_0^{2\pi} u(t)\cdot u(t-\tau)dt - 2\pi\bar{u}^2}{\int_0^{2\pi} u^2(t)dt - 2\pi\bar{u}^2}.$$

Since the function is periodic, we may change the intervals over which we are integrating to $-\pi$ to π.

$$cc_\tau(u,\tau) = \frac{\int_{-\pi}^{\pi} u(t)\cdot u(t-\tau)dt - 2\pi\bar{u}^2}{\int_{-\pi}^{\pi} u^2(t)dt - 2\pi\bar{u}^2}.$$

We take the Full Fourier Series for $u(t)$ over $(-\pi,\pi)$, so we have

$$u(t) = \frac{1}{2}A_0 + \sum_{n=1}^{\infty}(A_n\cos(nt) + B_n\sin(nt))$$

with $A_n = \frac{1}{\pi}\int_{-\pi}^{\pi} u(t)\cos(nt)dt$ and $B_n = \frac{1}{\pi}\int_{-\pi}^{\pi} u(t)\sin(nt)dt$ [21]. Also

$$u(t-\tau) = \frac{1}{2}A_0 + \sum_{n=1}^{\infty}(A_n\cos(n(t-\tau)) + B_n\sin(n(t-\tau)))$$

and we use $\cos(t-\tau) = \cos(t)\cos(\tau) + \sin(t)\sin(\tau)$ and $\sin(t-\tau) = \sin(t)\cos(\tau) - \cos(t)\sin(\tau)$. So now we can show the numerator of the cross correlation in terms of the Fourier Series

$$\int_{-\pi}^{\pi}\left[\frac{1}{2}A_0 + \sum_{n=1}^{\infty} A_n\cos(nt) + B_n\sin(nt)\right]\cdot$$
$$\left[\frac{1}{2}A_0 + \sum_{n=1}^{\infty}\cos(nt)(A_n\cos(n\tau) - B_n\sin(n\tau) + \sin(nt))(A_n\sin(n\tau) + B_n\cos(n\tau))\right]dt.$$

We now can simplify both the numerator and denominator. We can see that

$$\frac{1}{2}A_0 = \frac{1}{2\pi}\int_{-\pi}^{\pi} u(t)dt = \bar{u}.$$

Then, since

$$\int_{-\pi}^{\pi}\sin(nt)\cos(mt)dt = 0,$$

and also

$$\int_{-\pi}^{\pi} \sin(nt)\sin(mt)dt = 0,$$

and

$$\int_{-\pi}^{\pi} \cos(nt)\cos(mt)dt = 0,$$

for $n \neq m$ as well as

$$\int_{-\pi}^{\pi} \sin^2(nt)dt = \int_{-\pi}^{\pi} \cos^2(nt)dt = \pi,$$

When we multiply the two Fourier Series together, we are left with

$$\sum_{n=1}^{\infty} \left(A_n^2 \cos(n\tau) - A_n B_n \sin(n\tau) + A_n B_n \sin(n\tau) + B_n^2 \cos(n\tau)\right).$$

The denominator becomes

$$\sum_{n=1}^{\infty} [A_n^2 + B_n^2].$$

Thus our simplified cross correlation value is

$$cc_\tau(u, 2\pi) = \frac{\sum_{n=1}^{\infty} A_n^2 \cos(n\tau) + \sum_{n=1}^{\infty} B_n^2 \cos(n\tau)}{\sum_{n=1}^{\infty} [A_n^2 + B_n^2]}.$$

Now we want this to be equal to -1. So

$$\frac{\sum_{n=1}^{\infty} A_n^2 \cos(n\tau) + \sum_{n=1}^{\infty} B_n^2 \cos(n\tau)}{\sum_{n=1}^{\infty} [A_n^2 + B_n^2]} = -1$$

$$\sum_{n=1}^{\infty} A_n^2 \cos(n\tau) + \sum_{n=1}^{\infty} B_n^2 \cos(n\tau) = -\sum_{n=1}^{\infty} [A_n^2 + B_n^2].$$

$$\sum_{n=1}^{\infty} [A_n^2 + B_n^2](\cos(n\tau) + 1) = 0.$$

We know that $\cos(n\tau) + 1 \geq 0$ and $A_n^2 + B_n^2 \geq 0$. If we have $A_n^2 + B_n^2 = 0$ always hold then $u(t) = 0$, so we must have

$$\cos(n\tau) + 1 = 0$$

$$n\tau = (2k-1)\pi$$

$$\tau = \frac{(2k-1)\pi}{n}.$$

We make sure that $\frac{(2k-1)}{n}$ is in the most basic form, with $\gcd(2k-1, n) = 1$, and then we have our function $u(t)$ must be

$$u(t) = \sum_{m=1}^{\infty} [A_m \cos((2m-1)nt) + B_m \sin((2m-1)nt)]$$

with

$$\tau = \frac{(2k-1)\pi}{n}.$$

□

We can see as an example, that if $n = 2$ and $k = 2$ then $\tau = \dfrac{3\pi}{2}$. Then we have

$$u(t) = \sum_{m=1}^{\infty} [A_m \cos((4m+2)t) + B_m \sin((4m+2)t)].$$

The result we proved shows that only some special Fourier series can reach the cross correlation -1 even if all possible time shifts have been tried. For a periodic function arising from a nonlinear differential equation, this is unlikely to happen.

Chapter 4

Conclusions

We can draw a few conclusions from our work here. The diffusion coefficients have been shown to raise the cross correlation as it increases, meaning it raises the synchrony of the system. Additionally, the cross correlation appears to have a lower bound of around -0.5, with an upper bound of 1, while we also see that the average cross correlation over a number of time shifts is always 0.

When either or both of the coefficients a and b rise, the cross correlation spikes upward, as seen in the correlation plots, Figures $3.1 - 3.6$. This is not necessarily a linear rise, and specific values might lead to a greater spike than others, but without fail once the diffusion coefficients are high enough, the correlation value will be approach 1, the value for perfect synchrony. This agrees with the environmental view, as allowing for more interaction, or less isolation, between the two patches would lead to more similarities between the two in terms of populations.

The lower bound for the cross correlation tells us that there is no way to achieve antisychrony between the two patches. We showed in Chapter 3 the form an equation would have to take in order for there to be any possible antisynchrony. The presence of our diffusion terms would suggest that this makes sense, since the amount of movement is based on the difference in populations. The rates a and b that we set are based on the

difference in population of each patch, and so there is no way that all of one species can make it to the same patch.

While there are many dynamics that have an effect on the synchrony of predator and prey in multiple patches, we are able to say definitively that the diffusion rates have a positive correlation with synchrony. This can be added to the previously studied Moran effect as an understood cause of oscillations heading towards synchrony.

ACKNOWLEDGMENTS

I would like to thank William & Mary's Computational Science Training for Undergraduates in the Mathematical Sciences (CSUMS) for its support with CSUMS NSF Grant DMS-0703532 and The National Science Foundation for their support with NSF Grant DMS-1022648. Special thanks to my advisor Junping Shi and co-advisor Leah Shaw.

Bibliography

[1] E.M. Blalock, J.W. Geddes, K.C. Chen, N.M. Porter, W.R. Markesbery, and P.W. Landfield. Incipient Alzheimer's disease: microarray correlation analyses reveal major transcriptional and tumor suppressor responses. *Proceedings of the National Academy of Sciences of the United States of America*, 101(7):2173, 2004.

[2] E.A. Coddington and N. Levinson. *Theory of ordinary differential equations*. Tata McGraw-Hill Education, 1972.

[3] C. Elton and M. Nicholson. The ten-year cycle in numbers of the lynx in Canada. *The Journal of Animal Ecology*, pages 215–244, 1942.

[4] L. Glass. Synchronization and rhythmic processes in physiology. *Nature*, 410(6825):277–284, 2001.

[5] E.E. Goldwyn and A. Hastings. When can dispersal synchronize populations? *Theoretical population biology*, 73(3):395–402, 2008.

[6] E.E. Goldwyn and A. Hastings. Small heterogeneity has large effects on synchronization of ecological oscillators. *Bulletin of mathematical biology*, 71(1):130–144, 2009.

[7] A. Hastings. Transient dynamics and persistence of ecological systems. *Ecology Letters*, 4(3):215–220, 2001.

[8] C.S. Holling. The components of predation as revealed by a study of small-mammal predation of the European pine sawfly. *The Canadian Entomologist*, 91(5):293–320, 1959.

[9] P.J. Hudson and I.M. Cattadori. The Moran effect: a cause of population synchrony. *Trends in ecology & evolution*, 14(1):1, 1999.

[10] C.B. Huffaker. Experimental studies on predation: dispersion factors and predator-prey oscillations. *Hilgardia*, 27(14):343–383, 1958.

[11] W.D. Koenig. Global patterns of environmental synchrony and the Moran effect. *Ecography*, 25(3):283–288, 2002.

[12] I. Lengyel, I.R. Epstein, et al. Diffusion-induced instability in chemically reacting systems: Steady-state multiplicity, oscillation, and chaos. *Chaos (Woodbury, NY)*, 1(1):69, 1991.

[13] Y. Liu. *The Dynamical Behavior of a Two Patch Predator-prey Model.* Honors Thesis, College of William and Mary, 2010.

[14] A.J. Lotka. *Elements of physical biology.* Williams & Wilkins company, 1925.

[15] R.M. May. Limit cycles in predator-prey communities. *Science*, 177(4052):900, 1972.

[16] A. Pikovsky and M. Rosenblum. Synchronization. *Scholarpedia*, 2(12):1459, 2007.

[17] E. Ranta, V. Kaitala, J. Lindstrom, and E. Helle. The Moran effect and synchrony in population dynamics. *Oikos*, pages 136–142, 1997.

[18] J.L. Rodgers and W.A. Nicewander. Thirteen ways to look at the correlation coefficient. *American Statistician*, pages 59–66, 1988.

[19] M.L. Rosenzweig and R.H. MacArthur. Graphical representation and stability conditions of predator-prey interactions. *American Naturalist*, pages 209–223, 1963.

[20] T. Royama. *Analytical population dynamics*, volume 10. Springer, 1992.

[21] W.A. Strauss. *Partial differential equations-an introduction*. Wiley & Sons, Ltd, 1992.

[22] V. Volterra. Fluctuations in the abundance of a species considered mathematically. *Nature*, 118(2972):558–560, 1926.